Journal of the Serbian Chemical Society

QSAR studies of angiotensin converting enzyme inhibitors using CoMFA, CoMSIA and molecular docking

JIAN-BO TONG*, TIAN-HAO WANG, YI FENG and GUO-YAN JIANG

Shaanxi Key Laboratory of Chemical Additives for Industry, Shaanxi University of Science and Technology, Xi'an 710021, China

Abstract: In order to better understand the biochemical interactions governing their activities in lowering blood pressure, multiple quantitative structure-activity relationship (QSAR) models were developed from a data set of 58 angiotensin converting enzyme (ACE) inhibitors. The models were built by using comparative molecular field analysis (CoMFA) and comparative molecular similarity indices analysis (CoMSIA) techniques. The best CoMFA model had a cross-validation q^2 value of 0.940, a non cross-validation r^2 value of 0.952 and an external validation statistic Q_{ext}^2 value of 0.920. For the best CoMSIA model the values were with $q^2 = 0.872$, $r^2 = 0.926$ and $Q_{ext}^2 = 0.868$. Based on the contour maps, eight new ACE inhibitors were designed. Molecular docking was employed to further explore the binding requirements between the ligands and the receptor protein which included several hydrogen bonds between the ACE inhibitors and active site residues. This study showed extensive interactions between ACE inhibitors and residues of HIS383, GLU384, HIS513, TYR520 and LYS511 in the active site of ACE. The design of potent new inhibitors of ACE can get useful insights from these results.

Keywords: ACE inhibitors; 3D-QSAR; new drug design; molecular docking.

INTRODUCTION

Angiotensin converting enzyme (ACE) inhibitors play a key role in the regulation of peripheral blood pressure, mainly through the renin-angiotensin and kallikrein-kinin system.[1] ACE has been considered as a target in the prevention and treatment of hypertensive diseases.[2] It is generally believed that the absorption of 2-3 peptides from the gastro-intestinal tract of single stomach mammals is an important physiological phenomenon.[3] Therefore, ACE inhibitors peptides obtained more attention from researchers.

The explosive growth of information has resulted from a diversity of peptide studies. It has been difficult for scientists to identify the target molecule from

469

among the thousands of candidate compounds.[4] Although the traditional experimental method is relatively accurate, it is labor-intensive, time-consuming and costly. Therefore, scientists have sought new ways to address this problem.

QSAR is a method that is used to investigate the quantitative relationship between a series of compounds of related structure (including 2D/3D molecular and electronic structures) and biological activity (such as pharmaceutical activity, toxicity, and pharmacodynamics properties) by using theoretical calculations and statistical analytic tools.[5] The CoMFA and CoMSIA are especially effective methods based on statistical techniques. The CoMFA method was introduced by Cramer in 1987 and is widely used in the present practice of drug discovery. The advantage of CoMFA is its use in predicting the biological activity of molecules, taking into account the steric/electrostatic properties and biological activities and displaying the results in the form of contour maps.[6] CoMSIA is a more recently developed technique introduced by Klebe in 1994 and considers five different physicochemical properties: steric, electrostatic, hydrophobic, hydrogen bond donor (H bond donor) and hydrogen bond acceptor (H bond acceptor). The advantage of this method is that it considers more types of interactions, particularly hydrophobicity of compounds, than does CoMFA.[7] The two methods sample the potential fields surrounding a set of ligands and construct QSAR models by correlating these 3D fields with a common target receptor.

There were some papers studying the related issues of ACE inhibitors. Compared with references,[8–11] this study chose a new system consisting of 58 ACE inhibitors dipeptides for research, compared with reference,[12] this study used a new QSAR method for research. The present study aimed to develop predictive models and evaluate what structural features (hydrogen bond donor/acceptor, hydrophobic, steric and electrostatic) were responsible for the bioactivity of peptides.[13,14] These fields were mapped onto the inhibitors' binding pocket of ACE protease in order to better understand these interactions. Eight analogs of ACE inhibitors were designed as ACE protease inhibitors based on the molecular modeling candidates that had the highest biological activity. Molecular docking was selected to illustrate the binding mode between the ligands and the protein receptor. Surflex-dock results showed extensive interactions between ACE inhibitors and residues.

MATERIALS AND METHODS

Preparation of data set

A total of 58 ACE inhibitors peptides were selected from the published literature.[15] Each peptide was listed in Table I with a reported in vitro IC_{50} (the peptide concentration required to produce 50 % inhibition of ACE) value that was less than 1 mM. Before building the model, all IC_{50} values were converted to pIC_{50} values ($-\log (IC_{50}/\text{mmol L}^{-1})$). The structure and pIC_{50} values are shown in Table I. The whole data set was divided into two parts, a train-

ing set of 47 compounds that was used to construct the 3D-QSAR model and a test set of 11 compounds, that was used to evaluate capability of the model.

TABLE I. Amino acid sequences of 58 ACE inhibitors and their observed and predicted activities

| No. | Peptide | pIC_{50} | | | No. | Peptide | pIC_{50} | | |
| | | Observed | Predicred | | | | Observed | Predicted | |
			CoMFA	CoMSIA				CoMFA	CoMSIA
1	VW	5.80	5.71	5.51	30	KG	2.49	2.38	2.54
2	IW	5.70	5.59	5.64	31	FG	2.43	2.40	2.50
3	IY	5.43	5.35	4.79	32	GS	2.42	2.35	2.25
4	AW	5.00	5.05	5.01	33	GV	2.34	2.61	2.54
5	RW	4.80	5.01	4.83	34	MG	2.32	2.20	2.28
6	VY	4.66	4.42	4.76	35	GK	2.27	2.28	2.11
7	GW	4.52	4.65	4.78	36	GE	2.27	2.31	2.16
8	VF	4.28	4.17	4.00	37	GT	2.24	2.47	2.39
9	AY	4.06	3.93	4.22	38	WG	2.23	2.21	2.22
10	IP	3.89	3.76	3.72	39	HG	2.20	2.28	2.23
11	RP	3.74	3.82	3.63	40	GQ	2.15	2.31	2.19
12	AF	3.72	3.69	3.55	41	GG	2.14	2.18	2.17
13	GY	3.68	3.58	3.95	42	QG	2.13	2.11	2.12
14	AP	3.64	3.68	3.39	43	SG	2.07	2.38	2.09
15	RF	3.64	3.46	3.36	44	LG	2.06	2.03	2.38
16	VP	3.38	3.76	3.68	45	GD	2.04	1.90	2.06
17	GP	3.35	3.57	3.46	46	TG	2.00	2.28	2.09
18	GF	3.20	3.34	3.21	47	EG	2.00	1.90	1.97
19	IF	3.03	3.09	4.02	48[a]	DG	1.85	2.05	1.93
20	VG	2.96	2.90	2.98	49[a]	PG	1.77	1.95	2.07
21	IG	2.92	2.80	3.00	50[a]	LA	3.51	3.15	2.53
22	GI	2.92	2.72	2.56	51[a]	KA	3.42	3.54	2.68
23	GM	2.85	2.91	2.73	52[a]	RA	3.34	3.50	2.41
24	GA	2.70	2.32	2.31	53[a]	YA	3.34	3.60	2.69
25	YG	2.70	2.45	2.54	54[a]	AA	3.21	3.56	2.64
26	GL	2.60	2.73	2.71	55[a]	FR	3.04	3.49	2.77
27	AG	2.60	2.44	2.49	56[a]	HL	2.49	2.90	2.80
28	GH	2.51	2.60	2.69	57[a]	DA	2.42	2.12	2.08
29	GR	2.49	2.26	2.53	58[a]	EA	2.00	2.00	2.13

[a]Test set

Molecular modeling and alignment

The 3D-QSAR study was performed on SYBYL X-2.0. The 3D structures of all molecules were constructed using the Build Protein function. Partial atomic charges of all compounds were calculated by the Gasteiger–Huckel method, and then optimized for their geometry using Tripos field with a distance-dependent dielectric function and energy convergence criterion of 0.005 kcal*/(mol Å) using the maximum iterations set to 1000.[16,17] The

---

* 1 kcal = 4184 J

predictive accuracy and the reliability of the associated contour maps of such CoMFA and CoMSIA models are directly dependent on the molecular alignment.

Generally speaking, the lowest energy conformer of the most active peptide was selected as a template peptide. Based on the common structure, the residual peptides were aligned. In general, geometric similarity exists between the structure and the bioactive conformation for 3D-QSAR. Since the predictive capability of the model is directly dependent on alignment of molecules, selecting the common molecule structure is one of the important steps in performing 3D-QSAR analyses.[18]

CoMFA and CoMSIA analysis

The CoMFA and CoMSIA methods were employed to construct the predictive 3D-QSAR model based on aligned peptide drugs. In the CoMFA analysis, steric and electrostatic fields were calculated on a 3D grid with a spacing of 2.0 Å in *x*, *y*, and *z* directions for each of the alignments[19]. A sp³ carbon probe atom with a Lennard–Jones Coulomb radius of 1.52 Å and a charge of +1.00 was used as a probe to calculate the steric and electrostatic fields energy, respectively.[20] The cut-off value of steric and electrostatic fields was set to 30.0 kcal/mol. The St Dev* coefficients values as different weighing factors were performed to derive appropriate results. The model was used to get precise activity predictions of the untested compounds. The Lennard–Jones formula (1) and Coulomb formula (2) are as follows:

$$E_{vdW} = \sum_{i=1}^{n}(A_j r_{ij}^{-12} - C_j r_{ij}^{-6}) \tag{1}$$

$$E_C = \sum_{i=1}^{n} \frac{q_i q_j}{D r_{ij}} \tag{2}$$

For the CoMSIA analysis, similarity is expressed in terms of steric occupancy, electrostatic interactions, the standard settings of others at probe with charge +1, radius 1 Å, +1.0 for hydrophobic, hydrogen-bond donor and acceptor descriptors respectively.[21] CoMSIA can provide smooth and explicable contour maps using Gaussian-type distance dependence. In CoMFA and CoMSIA two or five descriptor fields are not totally independent of each other. CoMSIA calculates the similarity descriptors by way of a grid lattice. For a molecule *j* with atoms *i* at the grid point *q*, the CoMSIA similarity index AF is calculated by the equation (3):[22]

$$A_{F,K}^{q}(j) = -\sum_{i=1}^{n} w_{probe,k} w_{ik} e^{-ar_{iq}^2} \tag{3}$$

where w_{ik} is the actual value of the physicochemical property k of atom *i*; $w_{probe,k}$ is the property of the probe atom with a preset charge (+1 in this case), a radius (1.53 Å), and a hydrophobicity of 1; and r_{iq} is the mutual distance between the probe atom at grid point q and atom *i* of the molecule. In the CoMSIA calculations, five physicochemical properties (steric, electrostatic, hydrophobic, hydrogen bond donor, and hydrogen bond acceptor) were determined for all of the molecules.

Regression analysis by PLS method

In the present work, a partial least-squares (PLS) method, which is an extension of multiple regression analysis, was used to calculate the minimal set of grid points. And to correlate the CoMFA and CoMSIA fields to the experimental pIC_{50} values in order to generate the 3D-QSAR models. The leave-one-out (LOO) cross-validation was used to acquire the optimal number of components (*NC*) and the correlation coefficient (q^2).[23,24] The *NC* was then used to

produce the final QSAR model and to obtain the non-cross-validation correlation coefficient (r^2), standard error of estimate (*SEE*), the Fischer ratio value (*F*) and the contribution of steric (S) and electrostatic (E) fields. The CoMSIA model also can predict the contributions of hydrophobic (H), hydrogen bond donor (D) and hydrogen bond acceptor (A) fields. The CoMFA and CoMSIA results were then visually displayed in field contribution maps. Q_{ext}^2 indicates external validation statistics of the model. The q^2, formula (4), r^2, formula (5) and Q_{ext}^2, formula (6), are as follows:[25,26]

$$q^2 = 1 - \frac{\sum (Y_{obs} - Y_{pred})^2}{\sum (Y_{obs} - Y_{mean})^2} \tag{4}$$

$$r^2 = 1 - \frac{\sum (Y_{obs} - Y_{CVpred})^2}{\sum (Y_{obs} - Y_{mean})^2} \tag{5}$$

$$Q_{ext}^2 = 1 - \frac{\sum_{i=1}^{test} (Y_i - Y_{test})^2}{\sum_{i=1}^{test} (Y_i - Y_{trave})^2} \tag{6}$$

where Y_{mean} is the average activity value of the entire data set, while Y_{obs}, Y_{pred}, Y_{CVpred}, Y_{test} and Y_{trave} represent the observed values, predicted values, cross-validated activity values, test predicted activity values and training predicted activity values, respectively. High q^2, Q_{ext}^2 and r^2 values are considered to be indicators of the high predictive ability of the model.[27]

Molecular docking analysis

The research of the bonding between the enzyme and the ligands is meaningful for designing new drugs. The molecular docking investigations can explore the binding relationship between the ligands and the receptor protein.[28] In this paper, molecular docking was studied using Surflex-dock. The binding site was developed using the ACE X-ray with crystal structure (PDB ID: 1O86, www.rcsb.org) obtained from the RCSB Protein Data Bank. First, we analyzed the protein and fixed the side chains, and the terminal ends of the main chain. Then, 1O86 was prepared by adding hydrogen, adding charges, treating the terminal residues, and extracting the ligand.[29-31] Finally, the prototype molecule was generated. The molecule was docked into the active pocket.[32] The number of the maximum output poses was set as 20, and other set parameters were defaulted by SYBYL-X 2.0. The output poses were mainly evaluated by the total score.

RESULT AND DISCUSSION

CoMFA analysis of ACE inhibitors

The CoMFA and CoMSIA models were developed based on the set of 58 ACE inhibitors. The test set of 11 di-peptides (Table I) was employed to evaluate the reliability and applicability of the models. The most active peptide in the dataset was chosen as the template, *i.e.*, compound No. 1. The final superpositions of all peptides are displayed in Fig. 1.

Statistical parameters derived from the CoMFA model are summarized in Table II. The CoMFA model illustrates a cross-validated q^2 of 0.940, when using six components. The non-cross-validated PLS analysis resulted in a conventional $r^2 = 0.952$, $Q_{ext}^2 = 0.920$, $F = 91.363$, and *SEE* = 0.296. The values of pIC_{50}

predicted by CoMFA model are listed in Table I. A plot of calculated *versus* experimental activities for this model is shown in Fig. 2, which indicates the satisfactory predictive capability of the model. These data show that the performance of the model is moderately successful. The contributions of steric and electrostatic fields calculated by the CoMFA model are 74.4 and 25.6 % of variance, respectively, which indicates that steric fields make a slightly greater contribution in this model than do electrostatic.
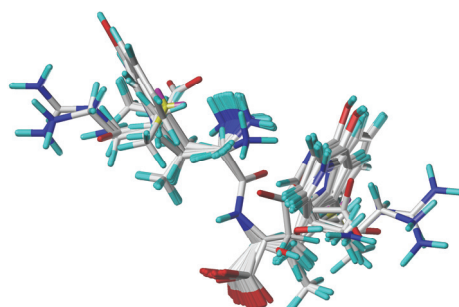

Fig. 1. The superpositions of peptides in the training and test sets of ACE inhibitors.

TABLE II. The statistical parameters for best 3D-QSAR models

| Field	Parameter					Contribution				
	q^2	NC	r^2	SEE	F	S	E	H	D	A
CoMFA										
SE	0.940	6	0.952	0.296	91.363	0.744	0.256	–	–	–
CoMSIA										
SEHDA	0.825	6	0.946	0.263	117.074	0.184	0.122	0.291	0.251	0.152
SEHD	0.872	6	0.926	0.260	120.728	0.217	0.161	0.327	0.295	–
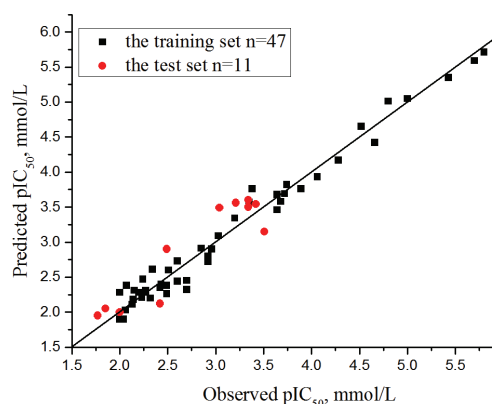
Fig. 2. Linear regression between experimental and predicted pIC_{50} values of ACE inhibitors.

The CoMFA analysis also gives contour plots of steric and electrostatic interactions. The steric interactions are represented by green-and yellow-colored contours in Fig. 3a. Bulky substituents in the regions shaded yellow are likely to

decrease biological activity, while bulky group substitutions in the green-colored regions are likely to enhance the activity. This is illustrated by the progressive reduction of activities of di-peptides in the series 25, 30 and 46 which have progressively smaller substituent volumes at the N-region. The same situation occurs in two other series of di-peptides, *i.e.*, 3, 6 and 13and 51, 53 and 24.
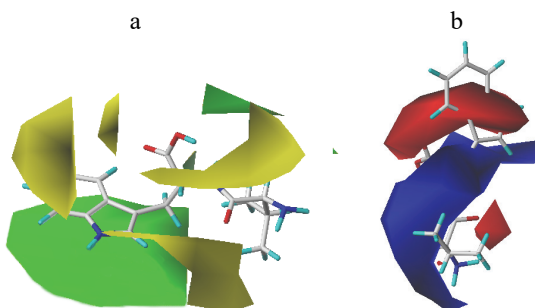

Fig. 3. CoMFA steric counter map (a) and electrostatic counter map (b).

Blue and red-colored contours in Fig. 3b represent the CoMFA electrostatic fields. Positively charged favorable blue regions are found around the N-terminal, while negatively charged favorable red regions are observed near the C-terminal, which could not indicate for its malposition. By comparing di-peptides 28, 29, 35 and 22, we see that the positive charge on the guanidino or ε-amino group of C-terminal Arg and His, as well as Lys side-chains, result in large reductions of potency. Overall, the CoMFA contour maps not only explain the QSAR of molecules, as reported, but also provide useful guidelines toward designing compounds for increased activity.

CoMSIA analysis for ACE peptides

The CoMSIA model was used to predict the activity of 58 ACE inhibitors. The best CoMSIA model was generated employing two alignment methods and different field combinations. There is no significant difference between the CoMSIA models developed by the database and field fit alignment methods. Therefore, the model generated by the database alignment that had a slightly higher cross-validated r^2 value was used for the final analysis. Based on this model, the correlation between experimental and predicted activity of all peptides is presented in Fig. 4, which indicate that there is no systematic error in the method. From Table II, the PLS analysis of the CoMSIA model was generated using steric, electrostatic, hydrophobic and hydrogen bond donor fields. It produced a cross-validated q^2 of 0.872 with an optimum number of six components and the corresponding non cross-validated $r^2 = 0.926$ with the *SEE* value = 0.260 and $F = 120.728$.
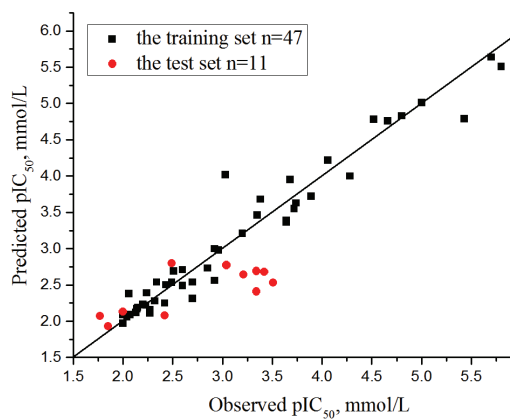
Fig. 4. Linear regression between experimental and predicted pIC_{50} values of ACE inhibitors by the best CoMSIA model.

The CoMSIA steric and electrostatic contour maps are shown in Fig. 5a and b.
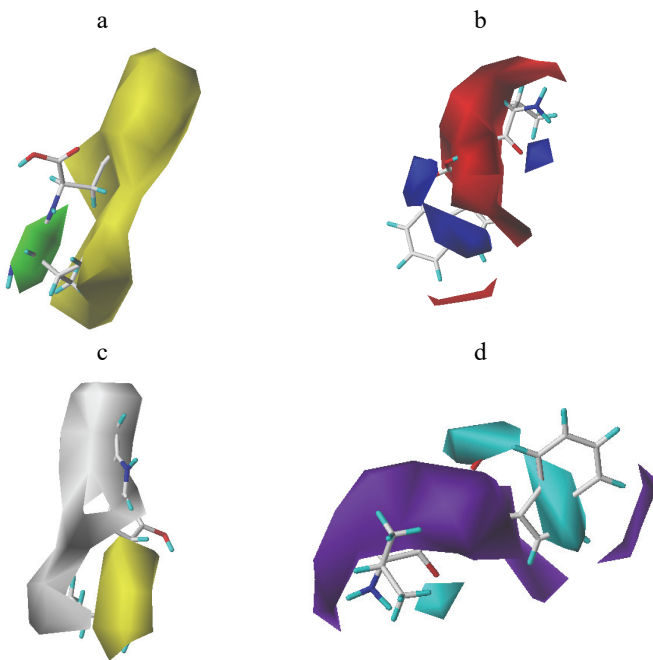
Fig. 5. CoMSIA contour maps: a) steric contour; b) electrostatic contour; c) hydrophobic contour; d) H-bond donor contour.

The contours are similar to the CoMFA steric and electrostatic contour maps. The CoMSIA hydrophobic contour map is shown in Fig. 5c. The yellow and gray contours indicate the regions where hydrophobic and hydrophilic groups are favored by the model, respectively. A large gray contour in the template molecule indicates that a change to a more a hydrophobic group will inc-

rease the activity, whereas the small yellow contour at the benzene ring indicates a position where a more hydrophilic group at this position will lead to increased activity. This trend is illustrated in the following series: 13 > 24; 51 > 52 > 24.

The CoMSIA hydrogen bond donor contour map is shown in Fig. 5d. The cyan contours represent the regions where hydrogen bond-donating groups increase the activity, whereas the purple contours represent the regions where hydrogen bond-donating groups decrease the activity. Fig. 5d shows purple contours around the C-terminal and N-terminal positions, indicating that a strong non-H bond donor group might increase the activity.

Drug molecular design

Based on the CoMFA and CoMSIA contour maps, we have designed 8 new compounds and predicted their activities using the CoMFA model. The structures and predicted activities (pIC_{50}) of 8 new compounds are displayed in Table III. The predicted activities of all the new compounds are higher than those of the training set molecules. This greater predicted activity may result from the fact that there is no bulky and electropositive substituent at the C-terminal position and a bulky substituent occupies the N-terminal of the molecules.

Table III. Structures and predicted pIC_{50} of newly designed molecules

No.	Structure	Predicted pIC_{50}
N1		5.990
N2		6.000
N3		5.840
N4		5.850
N5		6.210
N6		6.250
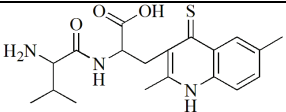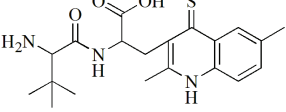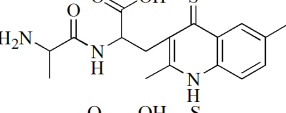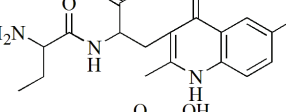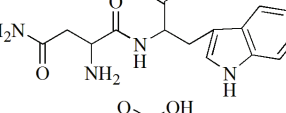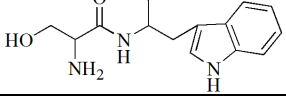
Table III. Continued

No.	Structure	Predicted pIC_{50}
N7		6.590
N8		6.220
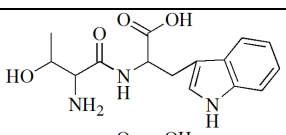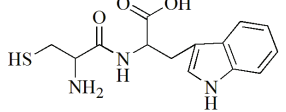
Docking study

Molecular docking study widely used to predict the potential binding mechanisms between the bioactive molecule and the target. In this study, Surflex-Dock was used to simulate the docking of ligands into the active site of target protein – renin. During this procedure, firstly, the selected ligand, A/LPR702, is extracted then all water molecules are removed, and finally the protein is hydrogenated. Aftar that the protomol (Fig. 6) is generated when the binding pocket is full of 3 molecular probes, *i.e.*, N–H, CH_4 and C=O, which represent hydrogen bond donor, hydrogen bond receptor, and hydrophobic sites, respectively.
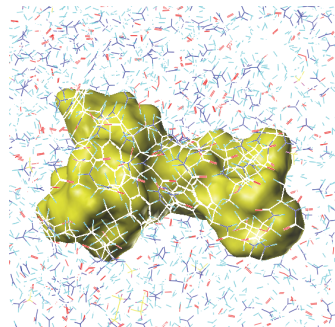

Fig. 6. Protomol (prototype molecule), which is generated when the binding pocket is full of 3 molecular probes, *i.e.*, N–H, CH_4 and C=O, respectively.

As shown in Fig. 7, compound No. 1 was selected to dock into the binding site of 1O86. The ligand is represented by sticks, the amino acid residues are represented by green lines, and the hydrogen bonds are represented by purple dotted lines. The compound No. 1 was the closest to these residues: ALA354, GLU384, HIS513, GLN281, TYR520 and LYS511. The distance between the hydrogen bonds formed by ALA354 is 1.588 Å (–O···H–), the distance between the hydrogen bonds formed by GLU384 is 2.065 Å (–O···H–), the distance between the hydrogen bonds formed by HIS513 is 2.065 Å (–N···H–), the distance between the hydrogen bonds formed by GLN281 is 2.053 Å (–H···O–), the distance between the hydrogen bonds formed by TYR520 is 1.876 Å (–H···O–),

the distance between the hydrogen bonds formed by LYS511 is 1.952 Å (–H···O–), respectively.
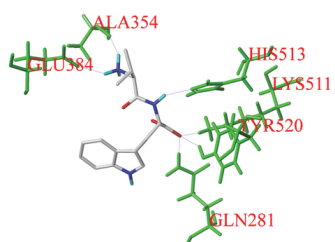

Fig. 7. The hydrogen-bond interaction between compound 1 and 1O86.

The total score containing crash score and polar score was total scoring function for the output pose of the molecules. In conclusion, the output pose was excellent when total score was more than 6.0. In this work, we used the total score method to screen the optimal pose. We have conducted molecular docking for the newly designed compounds and 1O86, then selected the results with the higher total score for analysis. The total-scores are shown in the Table IV. As shown in Fig. 8a–d, compounds N1, N5, N6 and N7 were docked into the active binding cavity of the ACE receptor.

Table IV. The results of molecular docking

No.	Total-score	Crash	Polar
N1	7.5498	−1.0749	4.4554
N2	6.8850	−2.2892	3.4409
N3	5.6833	−1.7477	3.4902
N4	6.9544	−1.3880	4.1844
N5	8.4445	−1.3372	7.0787
N6	7.5438	−0.8306	7.1443
N7	9.5820	−0.7493	7.4919
N8	7.0570	−0.6571	5.3465

In Fig. 8a, the designed new compound N1 has hydrogen-bonding interactions with HIS353, TYR523, GLU411, HIS387, HIS383 and GLU384. In Fig. 8b, the designed new compound N5 has hydrogen-bonding interactions with HIS513, TYR520, LYS511, GLN281, HIS353, ALA354, HIS387, HIS383 and GLU384. In Fig. 8c, the designed new compound N6 forms hydrogen-bonding interactions with GLN281, LYS511, HIS513, TYR520, ASP415, HIS383 and GLU384. In Fig. 8d, the designed new compound N7 forms hydrogen-bonding interactions with GLU384, GLN281, LYS511, TYR520, TYR523 and HIS513. Compound N7 has a high predicted activity (6.590) and high total-score value (9.5820), demonstrating that the compound is designed successfully.

The results showed that the ligand molecule has hydrogen bonding with the HIS383 residue, such as molecules N1, N5 and N6; the ligand molecule has hyd-

rogen bonding with the GLU384 residue, such as molecules N1, N5, N6 and N7; The ligand molecule has hydrogen bonding with the HIS513 residue, TYR520 residue and LYS511 residue, such as molecules N5, N6 and N7.
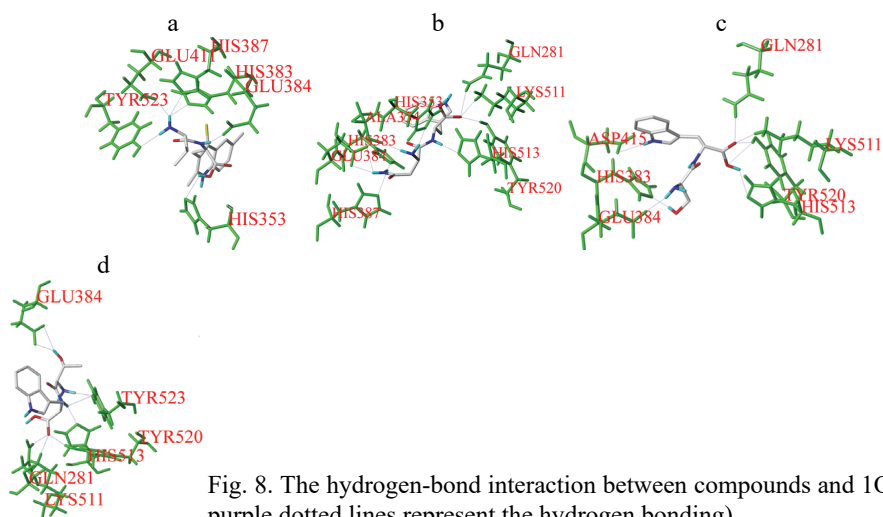

Fig. 8. The hydrogen-bond interaction between compounds and 1O86 (the purple dotted lines represent the hydrogen bonding).

All the newly designed compounds were docked in to 1O86, N3 had relatively low score value, so this compound is likely to be inappropriate. The docking results of the remaining new compounds N2, N4, and N8 with 1O86 were excellent, with the total score of 6.8850, 6.9544 and 7.0570, respectively, which showed that these docking conformations were useful to analyze as possible drug models.

CONCLUSION

In this study, 58 ACE inhibitors were studied using CoMFA and CoMSIA methods to generate 3D-QSAR models. Statistical parameters demonstrated that the established models are reliable and have a good internal and external predictive ability. The contour maps provide important relationships between structural features and inhibitory activities. Based on these contour maps, we designed new ACE inhibitors, all of which had higher activities than the training molecules. Finally, these new peptides and template molecules were used to simulate molecular docking. The results further indicated that the models are reliable and can be used to guide the development of new ACE inhibitor peptides.

И З В О Д

QSAR СТУДИЈЕ ИНХИБИТОРА АНГИОТЕНЗИН КОНВЕРТУЈУЋЕГ ЕНЗИМА КОРИСТЕЋИ CoMFA, CoMSIA И МОЛЕКУЛСКИ ДОКИНГ

JIAN-BO TONG, TIAN-HAO WANG, YI FENG и GUO-YAN JIANG

Shaanxi Key Laboratory of Chemical Additives for Industry, Shaanxi University of Science and Technology, Xi'an 710021, China

Да би се боље разумеле биохемијске интеракције које управљају њиховом активношћу у снижавању крвног притиска, развијен је модел вишеструке квантитативне релације сруктуре и активности (QSAR) на скупу података о 58 инхибитора ангиотензин конвертујућег ензима (ACE). Модели су изграђени користећи технике анализе компаративних молекулских поља (CoMFA) и индекса компаративне молекулске сличности (CoMSIA). Најбољи CoMFA модел има унакрсно валидацијску q^2 вредност 0,940, неунакрсно валидацијску r^2 вредност 0,952 и спољашњу статистичку Q_{ext}^2 вредност 0,920. За најбољи CoMSIA модел вредности су биле са $q^2 = 0,872$, $r^2 = 0,926$ и $Q_{ext}^2 = 0,868$. На основу контурних мапа дизајнирано је осам нових ACE инхибитора. Молекулски докинг је примењен да се даље истраже захтеви за везивање између лиганада и рецепторског протеина које укључују неколико водоничних веза између ACE инихибитора и остатака везивног места. Ова студија је показала значајне интеракције између ACE инхибитора и остатака HIS383, GLU384, HIS513, TYR520 и LYS511 у активном месту ACE. Резултати могу пружити корисне увиде за синтезу снажних нових инхибитора ACE.

(Примљено 16. јуна, ревидирано 31. јула, прихваћено 4. новембра 2020)

REFERENCES

1. B. L. Wang, D. Q. Pan, K. L. Zhou, Y. Y. Lou, J. H. Shi, *Spectrochim. Acta, A* **212** (2019) 15 (https://doi.org/10.1016/j.saa.2018.12.040)
2. M. F. Sperry, H. L. A. Silva, C. F. Balthazar, E. A. Esmerino, S. Verruck, E. S. Prudencio, R. P. C. Neto, M. I. B. Tavares, J. C. Peixoto, F. Nazzaro, R. S. Rocha, J. Moraes, A. S. G. Gomes, R. S. L. Raices, M. C. Silva, D. Granato, T. C. Pimentel, M. Q. Freitas, A. G. Cruz, *J. Funct. Foods* **45** (2018) 435 (https://doi.org/10.1016/j.jff.2018.04.015)
3. M. Yamaguchi, S. Hirai, T. Sumi, Y. Tanaka, M. Tada, Y. Nishii, T. Hasegawa, H. Uchida, G. Yamada, A. Watanabe, H. Takahashi, Y. Sakuma, *Biochem. Biophys. Res. Commun.* **487** (2017) 613 (https://doi.org/10.1016/j.bbrc.2017.04.102)
4. Z. I. Abu Hasan, H. Williams, N. M. Ismail, H. Othman, G. E. Cozier, K. R. Acharya, R. E. Isaac, *Sci. Rep.* **7** (2017) 45409 (https://doi.org/10.1038/srep45409)
5. P. Patel, H. Rajak, *Med. Chem. Res.* **27** (2018) 2100 (https://doi.org/10.1007/s00044-018-2219-4)
6. J. B. Tong, S. S. Qin, S. Lei, Y. Wang, *J. Serb. Chem. Soc.* **84** (2019) 303 (https://doi.org/10.2298/JSC180904098T)
7. S. Avram, D. Duda-Seiman, F. Borcan, P. Wolschann, *J. Serb. Chem. Soc.* **76** (2011) 263 (https://doi.org/10.2298/JSC100806022A)
8. T. Potter, H. Matter, *J. Med. Chem.* **41** (1998) 478 (https://doi.org/10.1021/jm9700878)
9. F. F. Wang, B. Zhou, *Mol. Divers.* (2019) (https://doi.org/10.1007/s11030-019-10005-0)
10. W. L. Yan, G. M. Lin, R. Zhang, Z. Liang, L. X. Wu, W. J. Wu, *J. Mol. Liq.* **304** (2020) 112702 (https://doi.org/10.1016/j.molliq.2020.112702)
11. A. A. S. Juan, S. J. Cho, *Bull. Korean Chem. Soc.* **26** (2005) 952 (https://doi.org/10.5012/bkcs.2005.26.6.952)

12. S. S. Liu, C. S. Yin, Z. L. Li, S. X. Cai, *J. Chem. Inf. Comput. Sci.* **41** (2001) 321 (https://doi.org/10.1021/ci0003350)
13. W. L. Jiang, Q. H. Chen, B. Zhou, F. F. Wang, *Med. Chem. Res.* **28** (2019) 1974 (https://doi.org/10.1007/s00044-019-02428-z)
14. M. Shu, T. Wu, B. W. Wang, J. Li, C. M. Xu, Z. H. Lin, *Chin. J. Struct. Chem.* **38** (2019) 7 (https://doi.org/10.14102/j.cnki.0254-5861.2011-1917)
15. E. R. Collantes, W. J. Dunn, *J. Med. Chem.* **38** (1995) 2705 (https://doi.org/10.1021/jm00014a022)
16. H. Zhi, J. X. Zheng, Y. Q. Chang, Q. G. Li, G. C. Liao, Q. Wang, P. H. Sun, *J. Mol. Struct.* **1098** (2015) 199 (https://doi.org/10.1016/j.molstruc.2015.06.004)
17. R. M. Asath, T. N. Rekha, S. Premkumar, T. Mathavan, A. M. F. Benial, *J. Mol. Struct.* **1125** (2016) 633 (https://doi.org/10.1016/j.molstruc.2016.07.064)
18. A. D. Beirami, Z. Hajimahdi, A. Zarghi, *J. Biomol. Struct. Dyn.* **37** (2019) 2999 (https://doi.org/10.1080/07391102.2018.1502687)
19. L. L. Wu, Y. Z. Wang, Y. Liu, S. Y. Yu, H. Xie, X. J. Shi, S. Qin, F. Ma, T. Z. Tan, J. P. Thiery, L. M. Chen, *Oncotarget.* **5** (2014) 7677 (https://doi.org/10.18632/oncotarget.2291)
20. H. Khani, M. B. Sepehrifar, S. Yarahmadian, *Med. Chem. Res.* **26** (2017) 1184 (https://doi.org/10.1007/s00044-017-1828-7)
21. V. C. Pham, M. J. Choi, T. W. Kim, J. Kim, D. J. Choo, K. T. Lee, J. Y. Lee, *Bull. Korean Chem. Soc.* **33** (2012) 305 (https://doi.org/10.5012/bkcs.2012.33.1.305)
22. Y. D. Liu, Y. W. Xie, Y. Y. Liu, P. C. Wang, J. X. Ye, Y. L. Su, Z. H. Liang, Z. H. He, H. B. Zhou, G. C. Zhou, J. Xu, Y. Q. Chang, P. H. Sun, *Med. Chem. Res.* **28** (2019) 1796 (https://doi.org/10.1007/s00044-019-02416-3)
23. E. Pourbasheer, R. Aalizadeh, *SAR QSAR Environ. Res.* **27** (2016) 385 (https://doi.org/10.1080/1062936X.2016.1184713)
24. G. Bringmann, C. Rummey, *Cheminform.* **43** (2003) 304 (https://doi.org/10.1021/ci025570s)
25. A. Singh, S. Goyal, S. Jamal, B. Subramani, M. Das, N. Admane, A. Grover, *Struct. Chem.* **27** (2016) 993 (https://doi.org/10.1007/s11224-015-0697-2)
26. J. B. Bhonsle, D. Venugopal, D. P. Huddler, A. J. Magill, R. P. Hicks, *J. Med. Chem.* **50** (2007) 6545 (https://doi.org/10.1021/jm070884y)
27. S. Yu, P. Wang, Y. Li, Y. Liu, G. Zhao, *SAR QSAR Environ. Res.* **24** (2013) 819 (https://doi.org/10.1080/1062936X.2013.820792)
28. P. P. Roy, J. T. Leonard, K. Roy, *Chemometr. Intell. Lab.* **90** (2008) 31 (https://doi.org/10.1016/j.chemolab.2007.07.004)
29. C. Xu, Y. J. Ren, *Bioorg. Med. Chem. Lett.* **25** (2015) 4522 (https://doi.org/10.1016/j.bmcl.2015.08.070)
30. D. D. Huang, Y. L. Liu, B. Z. Shi, Y. T. Li, G. X. Wang, G. Z. Liang, *J. Mol. Graphics Model.* **45** (2013) 65 (https://doi.org/10.1016/j.jmgm.2013.08.003)
31. J. B.Tong, Y. Wang, S. Lei, S. S. Qin, *Chin. J. Struct. Chem.* **38** (2019) 464 (https://doi.org/10.14102/j.cnki.0254-5861.2011-2123)
32. X. Q. Yan, Z. C. Wang, Z. Li, P. F. Wang, H. Y. Qiu, L. W. Chen, X. Y. Lu, P. C. Lv, H. L. Zhu, *Bioorg. Medl. Chem. Lett.* **25** (2015) 4664 (https://doi.org/10.1016/j.bmcl.2015.08.026).